# On the Nature of Equatorial Slant Sporadic *E*

ROBERT COHEN, KENNETH L. BOWLES, AND WYNNE CALVERT

*Central Radio Propagation Laboratory*
*National Bureau of Standards, Boulder, Colorado*

*Abstract.* Two features of the daytime sporadic *E* echoes observed on ionograms obtained near the magnetic equator have been termed 'equatorial sporadic *E*' and 'equatorial slant sporadic *E*.' These are traces that project from the *E*-layer trace and have equivalent ranges independent of frequency and proportional to frequency, respectively. Radar studies in Peru indicate that a thin stratum of magnetic-field-aligned irregularities embedded in the *E* layer is responsible for the entire sporadic *E* configuration. The increased equivalent ranges of the slant trace are attributed to oblique propagation in the east-west plane orthogonal to the irregularities. By accounting for the refraction and retardation imposed by the *E* layer, the entire configuration can be simulated in detail. It is established from this analysis that the equatorial electrojet flows within the equatorial *E* layer, and that its first-order current variations are coherent over distances of 500 km or more along the magnetic equator.

*Introduction.* The purpose of this paper is to explain the features of a common sporadic *E* configuration on daytime ionograms obtained near the magnetic equator.

Figure 1 is a typical daytime ionogram recorded at Huancayo, Peru (12°3'S, 75°20'W; magnetic dip, 2°N). Two regions of spread echoes from *E*-region heights have been classified in such ionograms as 'equatorial sporadic *E*' (*q* type) and 'equatorial slant sporadic *E*' (*s* type). The former is the somewhat diffuse trace which occurs at an equivalent range ($h'$) of about 100 km. The latter is the diffuse trace emerging from the former at a low frequency and rising in equivalent range with increasing frequency. No term has been adopted for the scatter echoes bounded by these two traces. The entire configuration of spread echoes is transparent to *F*-layer echoes. It will be shown to originate from a single thin stratum of scattering irregularities within the *E* layer.

Electron-density irregularities are encountered

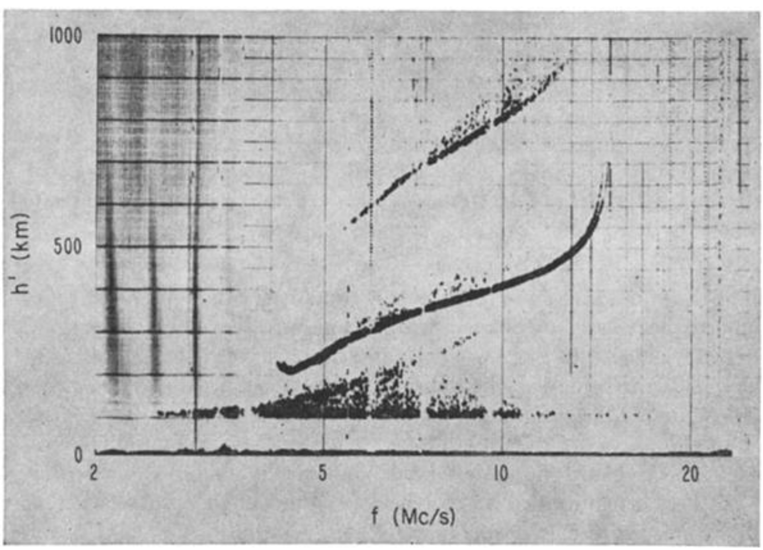


Fig. 1. Huancayo ionogram recorded at 1229 EST, April 19, 1960. It exhibits a typical equatorial slant sporadic *E*–equatorial sporadic *E* configuration.

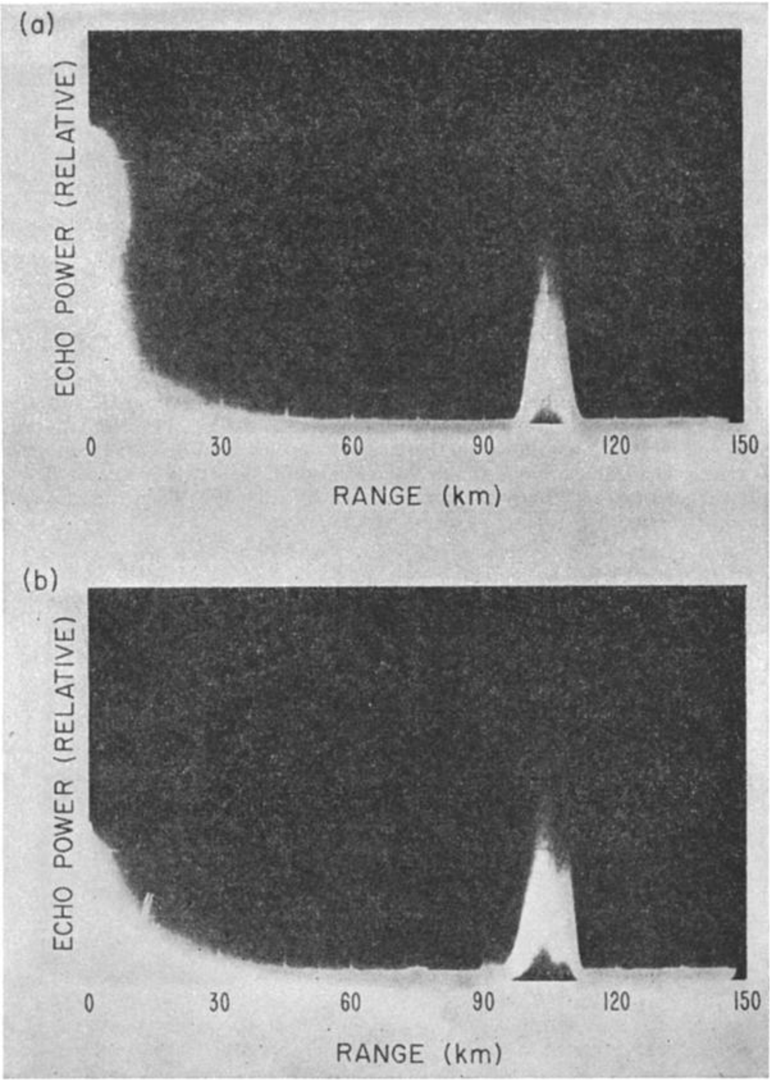


Fig. 2. Echoes from equatorial sporadic *E* irregularities at 50 Mc/s: (*a*) 1545 EST and (*b*) 1130 EST; Lima, Peru, April 18, 1961. A 10 microsecond (1.5 km) pulse width and a 100 kc/s bandwidth were employed.

in the *E* region of the equatorial ionosphere, and have been found to be closely associated with the equatorial electrojet current system [*Bowles and Cohen*, 1962]. These irregularities have been shown to be elongated and aligned with the earth's magnetic field (see next section). Using a scattering mechanism based upon observed characteristics of these irregularities, it will be shown how the various parts of the sporadic *E* configuration arise.

It is demonstrated in this paper that the equatorial sporadic *E* trace consists of echoes from irregularities that are more or less overhead, whereas the remainder of the spread echoes result from irregularities east and west of the station. The time delays associated with the equatorial slant sporadic *E* trace (and with the intermediate spread echoes) are imparted by (1) the oblique propagation and (2) refraction and retardation in the *E* layer en route to the scattering irregularities.

In this respect, the present model is similar

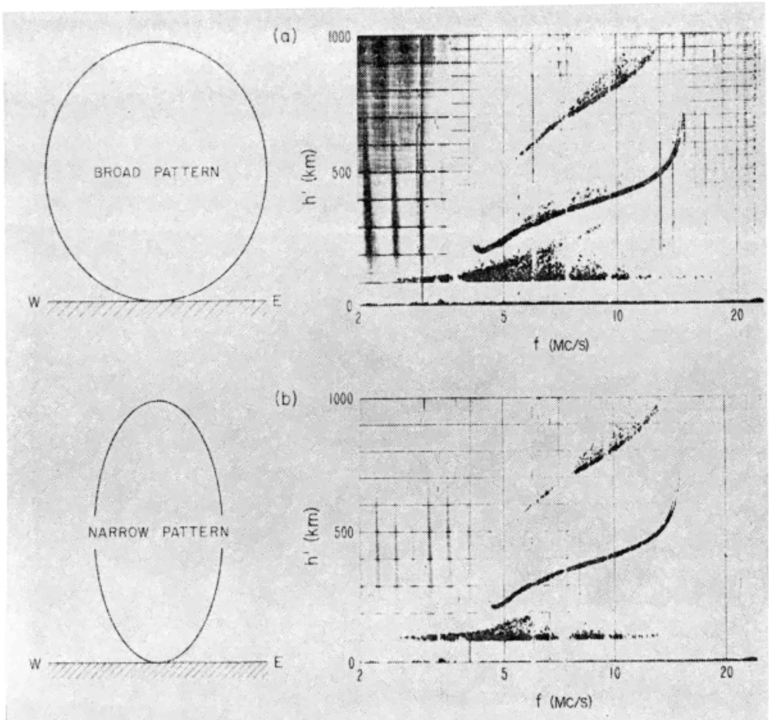


Fig. 3. The effect of antenna pattern changes upon equatorial sporadic *E* echoes at Huancayo: (*a*) 1229 EST and (*b*) 1231 EST; April 19, 1960. The log-periodic antenna arrays employed with the ionosonde had broad or narrow antenna patterns in the east-west plane, as indicated schematically on the left.

to those proposed by *Whale* [1951], *Smith* [1957], *Smith and Knecht* [1957], *Bates* [1961] (for auroral slant sporadic *E*), and *Renau* [1961].

The horizontal alignment of elongated irregularities at the magnetic equator limits scatter propagation to the vertical east-west plane through the ionosonde. This simplifies the calculation of ionograms for comparison with those observed.

*Experimental observations and interpretation.* *Egan* [1960] concluded from direction-of-arrival measurements that the irregularities he detected in the equatorial *E* region were aligned with the earth's magnetic field. Through the use of antenna lobing techniques, Bowles and Cohen (manuscript in preparation) confirmed this conclusion for the irregularities near 100 km giving rise to equatorial sporadic *E* echoes. *Bowles and Cohen* [1962] conclude also that the irregularities are of length 200 meters or greater, measured along the magnetic field lines, with at least one transverse dimension of the order of 6 meters or

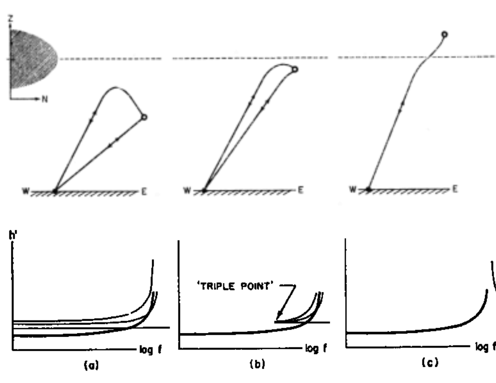


Fig. 4. Basic ray paths and the corresponding ionograms. The three cases are for a scattering irregularity situated (*a*) below the layer, (*b*) within the layer but below its height of maximum electron density, and (*c*) above that height. The calculations are based upon (1) ray theory, (2) horizontal stratification, (3) ordinary ray propagation in the vertical east-west plane, and (4) isotropic single-scattering normal to magnetic-field-aligned irregularities. The heavy trace is that of the usual *E*-layer echo.

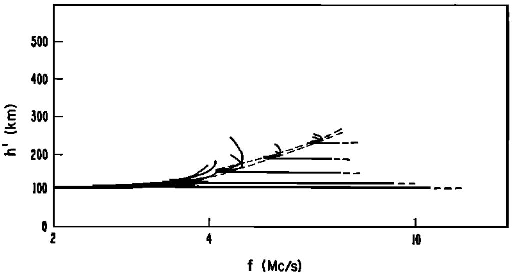


Fig. 5. Superposition of the individual ionograms corresponding to scatterers embedded in the $E$ layer below its height of maximum electron density. The scatterers are taken to be at a height of 105 km and at ground distances of 0, 50, 100, 150, and 200 km. The $E$ layer assumed for this figure and Figures 7, 8, and 10 is parabolic with its base at 100 km and a peak plasma frequency of 4.0 Mc/s at 114 km.

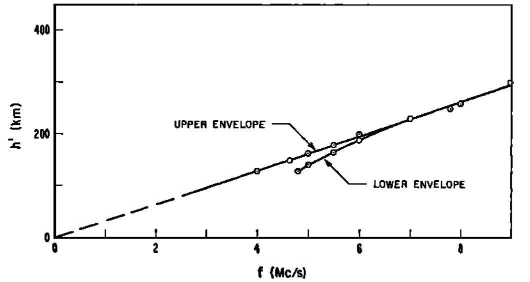


Fig. 6. The upper and lower envelopes of the equatorial slant sporadic $E$ trace of Figure 1, replotted with a linear frequency axis.

less. The irregularities are not circular in cross section, but may consist of a family of plane wave fronts whose wave normals are distributed in the plane perpendicular to the magnetic lines of force [*Bowles, Cohen, Ochs, and Balsley*, 1960].

Figure 2 shows an example of sporadic $E$ echoes received at 50 Mc/s using a highly directional antenna beamed vertically upward from Lima, Peru (11°57′S, 76°52′W; magnetic dip, 2°N). They generally extend from about 95 km to 110 km. There is no evidence of signals from higher up, even with the fairly large signal-to-noise ratios available. Thus the contention of *Egan* [1960] that the region in which equatorial sporadic $E$ irregularities occur extends from 100 km to 140 km in height and at times as high as 200 km does not appear to be well founded.

Further experimental information as to the origin of the scattered echoes appearing at virtual heights greater than 100 km has been obtained by the use of directional antennas in conjunction with the Huancayo ionosonde. These antennas were a pair of orthogonal log-periodic arrays. (Log-periodic antennas are constant in response over a considerable frequency range.) One was polarized north-south and had a broad beam pattern in the east-west plane; the other was polarized east-west and had a narrow beam pattern in the east-west plane. Figures 3*a* and 3*b*, recorded 2 minutes apart, are typical daytime ionograms obtained with these antennas. With the narrow east-west antenna pattern, the sporadic $E$ echoes at large time delays (including those near the 1$F$ trace) are diminished. On the other hand, the equatorial sporadic $E$ trace is unaffected on changing the beam pattern. Thus the equatorial sporadic $E$ trace results from essentially overhead scattering, while the equatorial slant sporadic $E$ trace (as well as the scatter echoes bounded by these traces) must result from scattering by irregularities east and west of the ionosonde. Hence the irregularities contributing to the scattering are those in a thin, horizontal, east-west band situated at $E$-region heights.

*The model.* The detailed appearance of the configurations on equatorial ionograms resulting from such a band of irregularities remains to be explained. The model to be employed here is based upon this band's being *embedded* in the equatorial $E$ layer. The frequency-dependent time delays of the scatter echoes result from oblique propagation and from refraction effects en route to a scattering irregularity in this band.

A refraction model similar to that adopted here has been used to describe configurations arising from equatorial spread $F$ irregularities

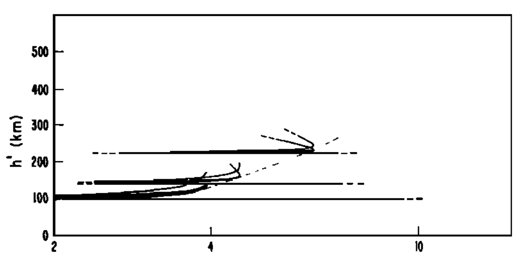


Fig. 7. Superposition of ionograms corresponding to scatterers situated below the $E$ layer. They are taken to be at a height of 99 km and at ground distances of 0, 100, and 200 km.

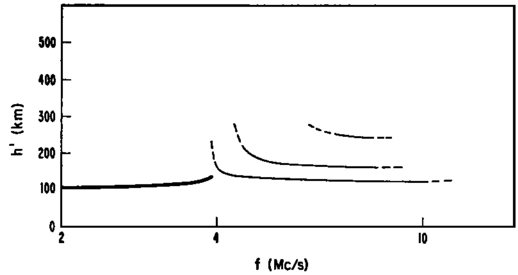


Fig. 8. Superposition of ionograms corresponding to scatterers situated above the height of maximum electron density of the *E* layer. They are taken to be at a height of 120 km and at ground distances of 0, 100, and 200 km.

[*Calvert and Cohen,* 1961]. The basic ray paths and corresponding ionograms for individual scattering irregularities were demonstrated to be those of Figure 4. The three cases correspond to an irregularity situated (*a*) below the refracting layer, (*b*) inside the layer below its height of maximum electron density, and (*c*) above that height. For (*a*) and (*b*), where there are two possible ray paths connecting the ionosonde and the scatterer, three scatter traces appear on the ionogram. They result from (1) direct backscatter, (2) reflected backscatter, and (3) scattering from one ray path into the other.

It will be shown below that the configuration of Figure 1 can be interpreted as a composite of 'ionograms'—like that of Figure 4*b*—corresponding to irregularities *embedded* in the equatorial *E* layer.

*Simulation of ionograms.* The approach to be followed here is to simulate observed configurations of scatter echoes by superimposing ionograms corresponding to individual irregularities appropriately located. The ultimate justification for the above model is the detailed correspondence that can be achieved between the calculated and observed ionograms. The result of such a simulation, for several irregularities located slightly above the base of the *E* layer and distributed east or west of the ionosonde, is shown in Figure 5.

Simulations of this sort can not only reproduce the observed configurations, but can also predict the presence of latent features on the ionogram that may have escaped notice. For example, the equatorial slant sporadic *E* trace of Figure 5 has a definite width that decreases with increasing frequency. This feature can also be noted in Figure 1. The upper envelope is generated by the 'triple points' (cf. Fig. 4*b*) of the echo configurations for the individual irregularities. The locus of such triple points has been shown to be

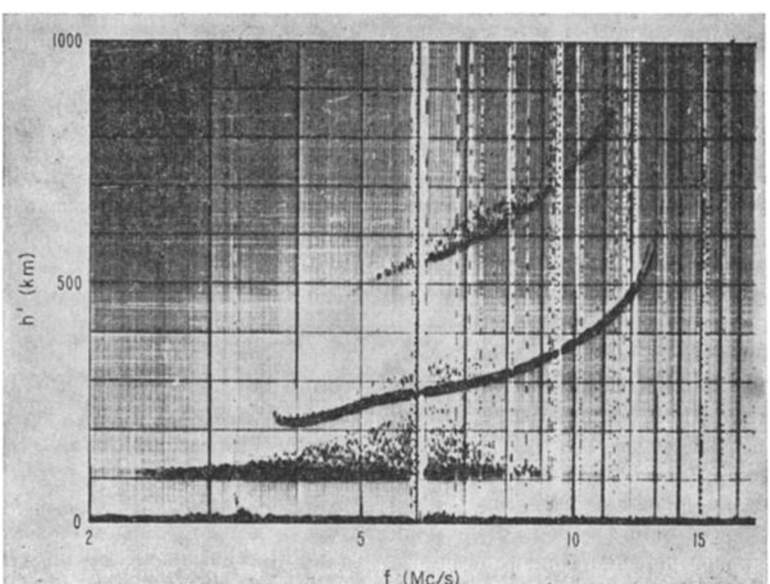


Fig. 9. Huancayo ionogram recorded at 0915 EST, April 3, 1960. In this case the equatorial slant sporadic *E* trace is not enhanced.

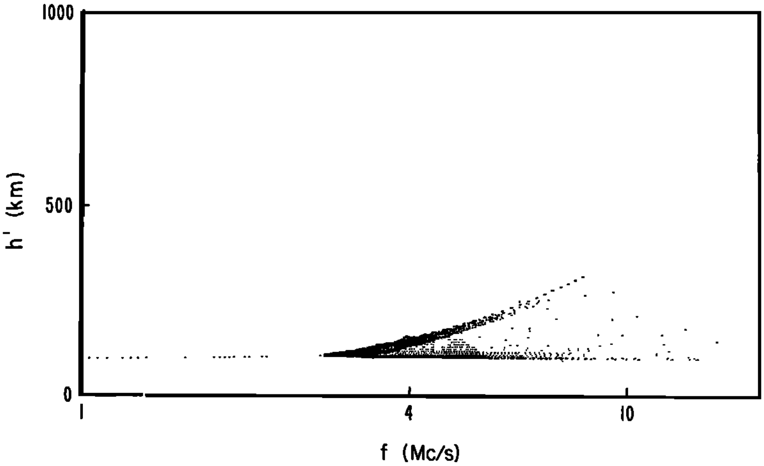


Fig. 10. Simulation of the equatorial sporadic $E$ configuration. Scattering irregularities were assumed to be at a height of 105 km (as in Fig. 5) and to extend as far as 300 km on either side of the ionosonde. The separations of points is adjusted (beyond a cutoff) to be inversely proportional to the expected echo intensity (varying as $(f \sin \theta/2)^{-3}h'^{-3}$).

linear—that is, it has an equivalent range proportional to frequency [*Calvert and Cohen*, 1961]. It is expected to be accentuated on the ionogram since it results from scattering at the ray reflection level, where the density of rays is enhanced. The lower envelope is generated by the center traces of the triplets, being their caustic focus. Furthermore, the center traces are enhanced in comparison with the other traces because they involve a smaller scattering angle. (The two envelopes converge with increasing frequency, although it can be shown that this coalescence will not continue indefinitely.)

The linearity of slant sporadic $E$ traces has been observed by Agy (private communication to *Smith and Knecht* [1957]) and by *Whale* [1951]. This property of the equatorial slant sporadic $E$ trace is exhibited in Figure 6. (Note in this figure that it is the equivalent range of the *upper* envelope which is linear.)

Figure 5 may be contrasted with the results of similar computations for hypothetical irregularities situated below the layer (Fig. 7) and above the height of maximum electron density (Fig. 8). Huancayo ionograms resembling Figure 7 (showing a lower slant envelope without an upper slant envelope) do not seem to occur, so it is concluded that the stratum of irregularities does not occur below the $E$ layer. However, the configuration of Figure 8 may correspond to periods when the equatorial slant sporadic $E$ is poorly defined, as in Figure 9. This suggests that the stratum of irregularities may, at times, extend above the height of maximum electron density of the $E$ layer.

*Simulation of ionogram intensity.* In the process of ionogram simulation described above, a small number of scatterers have been considered in order to maintain the identity of the triplets of scatter traces. Furthermore, the extensions of these triplets along the frequency axis have been arbitrarily terminated. It is possible, however, to take into account the relative scatter amplitude associated with each point of the triplet. The number density of points plotted from the ray computations can then be adjusted in accordance with these amplitudes, providing a graphical simulation of the ionogram intensity.

On most theoretical treatments, the power scattered at a frequency $f$, through a scattering angle $\theta$, is proportional to the parameter $f \sin (\theta/2)$ raised to some negative exponent. There is reason to believe that this exponent varies with frequency, being about 9.4 in the range 4 to 8 Mc/s [*Skinner and Wright*, 1961], but becoming about 3 at higher frequencies [*Bowles and Cohen*, 1962].

The echo power is estimated to vary with distance as $h'^{-3}$. This factor takes into account

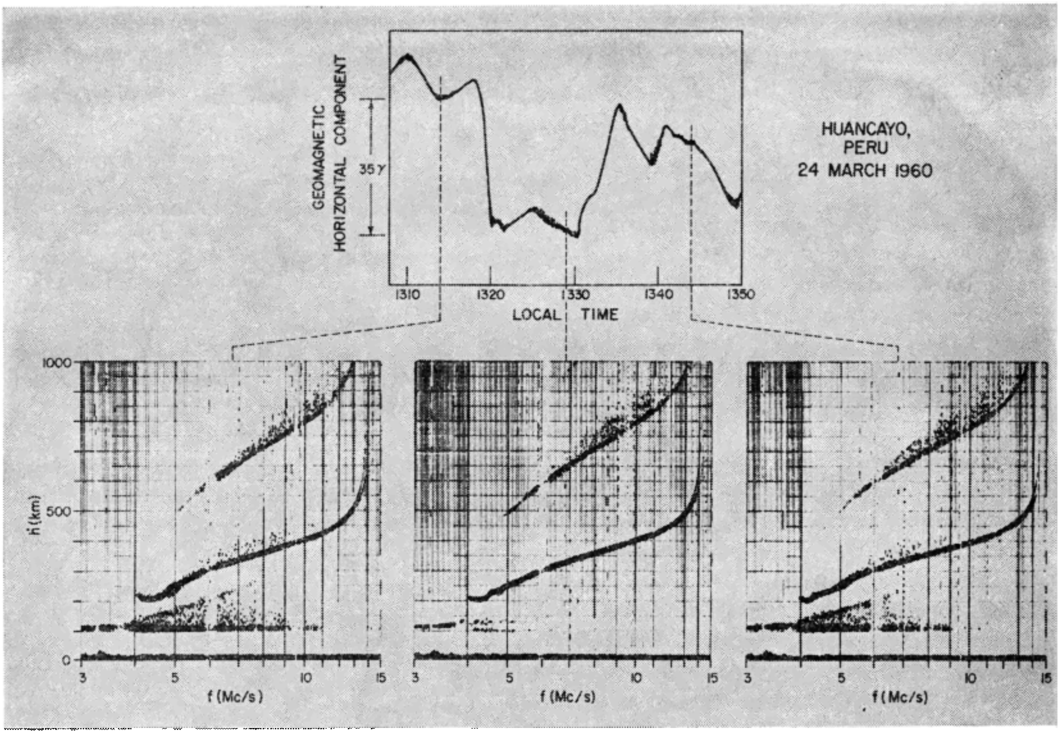


Fig. 11. Association of equatorial sporadic *E* irregularities and the equatorial electrojet current. The diminution of the geomagnetic *H* component (and hence the electrojet) is coincident with the disappearance of the equatorial sporadic *E* configuration. These observations were performed at Huancayo, 1314 EST to 1344 EST, March 24, 1960.

the size of the Fresnel zone in the north-south direction and the spreading of the rays in the vertical east-west plane.

Figure 10 was produced using these two simple estimates for the echo power. The *E* layer was taken to be parabolic, 28 km thick, with maximum electron density at 114 km. An east-west band of scattering irregularities was assumed, at a height of 105 km and extending as far as 300 km (ground distance) on either side of the ionosonde. The scattering exponent was assumed to be 3.0. This low value was chosen in order to compensate (in a crude manner) for two omitted factors: *D*-layer absorption and possible loss in antenna gain at lower frequencies.

*Equatorial electrojet.* The close association of the equatorial sporadic *E* irregularities and the equatorial electrojet (Cohen and Bowles, manuscript in preparation) is demonstrated in Figure 11. This figure shows the positive correlation of the horizontal component (*H*) of the magnetic field at Huancayo with the development of the equatorial sporadic *E* configuration. (*H* is a measure of the current density in the electrojet.)

Since the irregularities east or west of the ionosonde contribute echoes at greater equivalent ranges than do those overhead, the fact that the equatorial sporadic *E* configuration always disappears as a unit implies that there is considerable coherence along the magnetic equator in the variations of the electrojet current. Inasmuch as the greatest observed equivalent range of slant traces corresponds to horizontal separations of 250 km or so, this coherence extends at least 500 km.

It is noted that the equatorial slant sporadic *E* trace is more or less accentuated from time to time. As has been demonstrated, the degree of its accentuation can be explained by the relative height of the stratum of irregularities (i.e., probably identical to the height of the electrojet) with respect to the height of the *E* layer.

*Conclusions.* 1. The entire daytime configuration of sporadic *E* echoes observed on equatorial ionograms is due to a thin stratum of magnetic-field-aligned irregularities *embedded* in the equatorial $E$ layer.

2. The equatorial slant sporadic $E$ trace arises by a mechanism involving propagation in the vertical east-west plane and scattering from these irregularities.

3. The degree of accentuation of this trace is indicative of whether or not the stratum of irregularities extends above $h_{max}$.

4. The characteristic appearance of the equatorial sporadic $E$ configuration establishes that this stratum cannot extend below the base of the equatorial $E$ layer.

5. Since the magnetic-field-aligned irregularities are associated with the equatorial electrojet, conclusions 3 and 4 mean that the electrojet itself may sometimes flow above $h_{max}$ but that it does not flow below the equatorial $E$ layer.

6. The fact that the equatorial sporadic $E$ configuration always disappears as a unit implies an east-west coherence over at least 500 km along the magnetic equator of the first-order current variations of the equatorial electrojet.

*Acknowledgments.* The collaboration of G. R. Ochs, J. R. Winkelman, and J. T. Brown, Jr., of NBS and of A. A. Giesecke, Jr., Director-Técnico, M. Tábara, J. Lanat, and H. Goller of the Instituto Geofísico del Perú is gratefully acknowledged.

## References

Bates, Howard F., The slant $E_s$ echo—a high-frequency auroral echo, *J. Geophys. Research, 66,* 447–454, 1961.

Bowles, Kenneth L., and Robert Cohen, A study of radio wave scattering from sporadic $E$ near the magnetic equator, in *Ionospheric Sporadic E,* Pergamon Press, in press, 1962.

Bowles, K. L., R. Cohen, G. R. Ochs, and B. B. Balsley, Radio echoes from field-aligned ionization above the magnetic equator and their resemblance to auroral echoes, *J. Geophys. Research, 65,* 1853–1855, 1960.

Calvert, Wynne, and Robert Cohen, The interpretation and synthesis of certain spread-$F$ configurations appearing on equatorial ionograms, *J. Geophys. Research, 66,* 3125–3140, 1961.

Egan, R. D., Anisotropic field-aligned ionization irregularities in the ionosphere near the magnetic equator, *J. Geophys. Research, 65,* 2343–2358, 1960.

Renau, Jacques, Theory of overhead nonblanketing sporadic *E, J. Geophys. Research, 66,* 2121–2128, 1961.

Skinner, N. J., and R. W. Wright, The reflection coefficient and fading characteristics of signals returned from the $E_s$ layer at Ibadan, in *Ionospheric Sporadic E,* Pergamon Press, in press, 1962.

Smith, Ernest K., Jr., National Bureau of Standards Circular 582, *Worldwide Occurrence of Sporadic E,* U. S. Government Printing Office, Washington, 1957 (originally issued as an unpublished NBS report in 1955).

Smith, E. K., and R. W. Knecht, Some implications of slant-$E_s$, *J. Atmospheric and Terrest. Phys.,* Spec. Suppl., part 2, 195–204, 1957.

Whale, H. A., Fine structure of the ionospheric region *E, J. Atmospheric and Terrest. Phys., 1,* 233–243, 1951.

(Manuscript received December 22, 1961.)